Corrosion Behaviour of Cold Rolled Steel in 84 Disinfectant Solutions

Qing Qu[1,], Rui Yuan[1], Lei Li[2], Yunwei He[1], Jun Luo[2], Lei Wang[1], Hangtian Xu[2], Yanyan Gao[1], Yanru Song[1], Zhongtao Ding[1]*

[1] School of Chemical Science and Technology, Yunnan University, Kunming 650091, China
[2] Laboratory for Conservation and Utilization of Bio-Resources, Yunnan University, Kunming 650091, China
[*]E-mail: quqing@ynu.edu.cn; quqing58@126.com

Corrosion behaviour of cold rolled steel in different concentrations of 84 disinfectant was studied by gravimetric measurements, Tafel polarization curves, and electrochemical impedance spectroscopy. Concentrations of 84 disinfectant and temperature have a strong acceleration effect. Both the anodic dissolution and cathodic reduction can be speeded up by 84 disinfectant. The corrosion rate increases with increasing temperature, but does not increase with increasing the concentration all the way; the maximum corrosion rate appears at 20 mL/L 84 disinfectant. The result of chemical experiments shows that Fe^{3+} ions are the dominant corrosion products dissolved in 84 disinfectant solutions due to the strong oxidation of 84 disinfectant. Atomic force microscopy indicates that protective film forms when concentration of 84 disinfectant is equal to 20 mL/L.

1. INTRODUCTION

Carbon steels are commercially available metals, which are used in the fabrication of reaction vessels, storage tanks, etc. Corrosion behaviour of steels is widely investigated in inorganic acids [1-3], salts [4], non-oxidation organic acids [5], alkaline solutions [6], and marine media [7,8], and many inhibitors were also suggested to retard the corrosion of steel in the above-mentioned solutions [9-15]. However, corrosion behaviour and corrosion inhibition of carbon steel in oxidation media, especially in strong oxidizing disinfectant solutions were rather scant [16,17]. Strong oxidizing disinfectant solutions have wide range of biocidal activity; they can be used to kill bacteria, algae, yeasts, moulds, fungi and viruses. The most commonly used disinfectant method is chlorination which can be either

electrolytically produced or added to generate hypochlorite compounds (e.g., sodium hypochlorite). Thus, many solutions containing sodium hypochlorite are used as disinfectants, among them, a new-fashioned chlorinated disinfectant named 84 disinfectant, is made from sodium hypochlorite and surface active agent [18-20]. Dilution of 84 disinfectant is usually used for disinfection of hospitals, factories and homes [18-20]. However, major disadvantages associated with 84 disinfectant are the serious economic loss due to its highly corrosive capability to many metals such as aluminium, carbon steel [18-20], which are used in some appliances in family and hospital. But to date, there is little available data on the corrosion behaviour of metals in solutions containing 84 disinfectant, the corrosion mechanism of metals in 84 disinfectant solutions is unclear which results in the shortage of high-efficient inhibitors, accordingly, the practical application of 84 disinfectant is also limited. Therefore, it is interesting in studying the corrosion regularities of metals in solutions containing 84 disinfectant in order to develop some high-efficient inhibitors.

In the present work, the corrosion behaviour of cold rolled steel (CRS) in 84 disinfectant solutions is investigated by gravimetric measurements, Tafel polarization curves, and electrochemical impedance spectroscopy. Effects of concentration of 84 disinfectant and temperature on the corrosion rate are also discussed in detail. A probable corrosion mechanism is presented to explain the related experimental results. Atomic force microscopy (AFM) is used to characterize the corrosion surface to ascertain the corrosion mechanism.

2. EXPERIMENTAL PROCEDURES

2.1. Materials

The working electrodes were made of a sheet of cold rolled steel (CRS), which was of commercial specification with composition (wt.%): C ≤ 0.05, Si ≤ 0.02, Mn ≤ 0.28, S ≤ 0.023, P ≤ 0.019, Fe remainder.

2.2. Solutions

84 disinfectant used in this work was produced by Guangzhou blue moon industrial Co. The main active ingredient of 84 disinfectant is sodium hypochlorite which concentration is about 10000 mg/L. The aggressive solution, 2, 3.3, 10, 20, 40, 100 mL/L 84 disinfectant were prepared by dilution of 84 disinfectant solution from distilled water by volume, respectively. To further elucidate the strong corrosivity of 84 disinfectant, distilled water also was used as the control experiment.

2.3. Gravimetric measurements

Prior to experiments, three parallel CRS sheets of 40 × 10 × 5 mm size were successively abraded using emery papers from 100 to 1000 grade. Then, the specimens were washed with distilled water and degreased with acetone and dried with a cold air blaster. After weighing accurately, the

specimens were immersed in 250 mL beakers containing different concentrations of 84 disinfectant solutions for 4 h at 10, 20, 30, 40 °C, respectively. The samples were then taken out and subsequently immersed in ASTMG1-90 standard solution (Clark solution: 100 mL HCl + 2 % Sb_2O_3 + 5% $SnCl_2$) to remove the corrosion products, then washed with distilled water and acetone, dried and reweighed accurately.

2.4. Electrochemical measurements

A three-electrode system including a working electrode, an auxiliary electrode and a reference electrode was used for the electrochemical measurements in 250 mL solution. The working electrodes were made of CRS which were embedded in PVC holder using epoxy resin with a square surface of 1.0 cm^2. The auxiliary electrode was a platinum foil. The reference electrode was a saturated calomel electrode (SCE) with a fine Luggin capillary positioned close to the working electrode surface in order to minimize ohmic potential drop. Each specimen was successively abraded by using SiC emery papers from 100 to 1000 grades on the test face. Before use, the abraded surface was thoroughly washed with distilled water and degreased in acetone then dried with a warm air stream. The working electrode was immersed in the test solution at open circuit potential for 2 h before measurement until a steady state appeared. Tafel polarization curves were determined by polarizing to ±250 mV with respect to the free corrosion potential (E_{corr} vs. SCE) at a scan rate of 0.5 mV/s. A 10 mV peak to-peak sine wave over an ac frequency range extending from 0.1 Hz to 100 kHz was used for the impedance measurements. All electrochemical measurements were carried out at the open circuit potential using PARSTAT 2263 Potentiostat/Galvanostat (Princeton Applied Research). Each experiment was repeated at least three times to check the reproducibility. All tests have been performed in non-deaerated solutions under unstirred conditions at 10 - 40 °C.

2.5. AFM studies

Before monitoring the topographic changes of electrode surface, the specimens were abraded with emery paper from 100 to 1000 grade, and then washed with distilled water and acetone. After immersion in different concentrations of 84 disinfectant at 30 °C for 4 h, the specimens were washed with distilled water and degreased in acetone then dried with a warm air stream. Then the surface morphologies of CRS specimens were studied by a SPA-400 AFM (Seiko Instrument Inc.).

3. EXPERIMENTAL RESULTS

3.1. Gravimetric measurements

The average weight loss of the CRS specimens as a function of concentration of 84 disinfectant after 4 h immersion at 10 – 40 °C at were shown in Fig. 1. It is apparent from this figure that, at each temperature, the average weight loss of CRS does not increase all the way with increasing

concentration of 84 disinfectant, the average weight loss obviously increases with increasing 84 disinfectant concentration when concentration of 84 disinfectant is lower than 20 mL/L, but the situation is the opposite when the concentration is equal or higher than 20 mL/L. That is, the maximum corrosion rate of CRS appears at the ratio of 20 mL/L 84 disinfectant at each temperature.
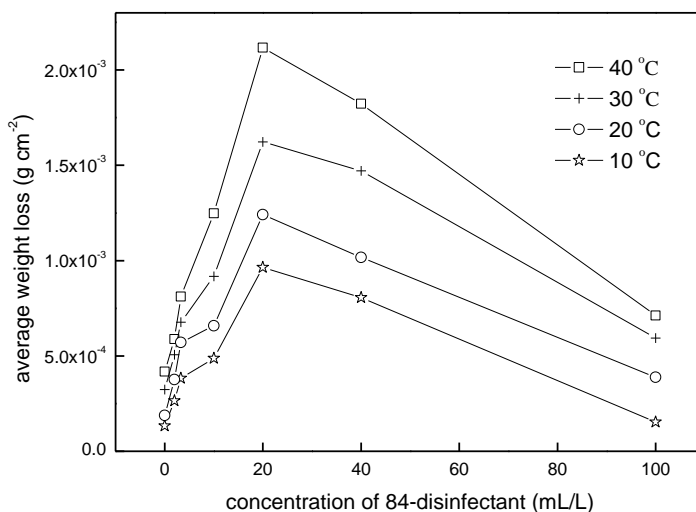

Figure 1. Average weight loss of CRS in different concentrations of 84 disinfectant at different temperatures.

Figure 1 also indicates that, with increasing the temperature from 10 to 40 °C, the average weight loss of the CRS increases at each same concentration of 84 disinfectant, which is in good agreement with the theory of chemical kinetics. To further discuss the effect of temperature, the dependence of the corrosion rate on temperature was expressed by the Arrhenius equation:

$$v = A \exp\left(\frac{-E_a}{RT}\right) \qquad\qquad (1)$$

where v is the corrosion rate in g cm^{-2} h^{-1}, A is the pre-exponential factor in g cm^{-2} h^{-1}, E_a is the activation energy of the metal corrosion reaction in J mol^{-1}, R is the gas constant and T the temperature.

Converting Eq. (3) to ordinary logarithms gives

$$\ln v = \ln A - \frac{E_a}{RT} \qquad\qquad (2)$$

When ln$v$ is plotted on the vertical axis against $1/T$ on the horizontal, a straight line should result.

Figure 2 shows the Arrhenius plots for the corrosion of CRS with and without 84-disinfectant. The results give rise to satisfactory straight lines with slopes of ($-E_a / R$). The calculated values of E_a from the slopes are found to be 29.3, 19.9, 18.0, 17.4, 19.3, 20.8, 37.5 kJ mol^{-1} for the solutions in the presence of 0, 2, 3.3, 10, 20, 40 100 mL/L 84-disinfectant, respectively. In general, E_a decreases with increasing the concentration of 84 disinfectant from 0 to 20 mL/L, then increases with increasing the

concentration of 84 disinfectant from 20 to 100 mL/L, which further indicates that the maximum corrosion rate appears at 20 mL/L.
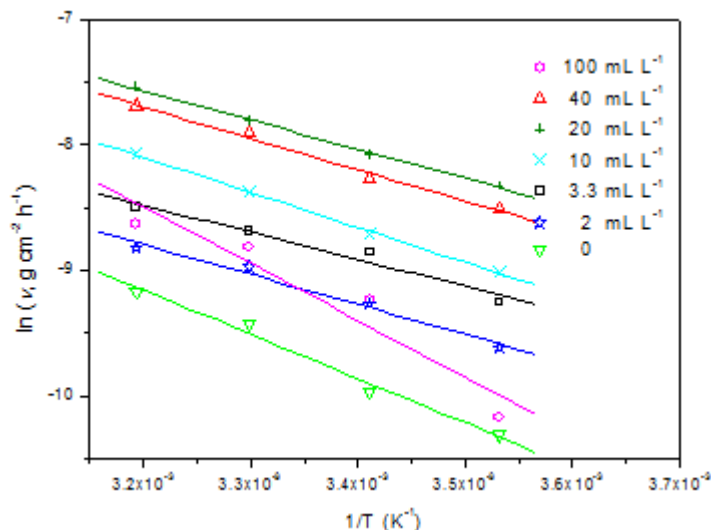

Figure 2. Arrhenius plots of lnν versus *1/T* for CRS in different concentrations of 84 disinfectant.

According to Fu et al. [21], values of E_a up to 100 kJ mol^{-1} are consistent with the slow reaction that should be heated, while those less than 40 kJ mol^{-1} involve the reaction that can quickly take place at room temperature. In our case, all the values of E_a are lower than 40 kJ mol^{-1}, meaning that corrosion of CRS in solution with 84 disinfectant occurs easily.

3.2 Tafel polarization

Figs.3a-d present the polarization curves of CRS exposed to different concentrations of 84 disinfectant at test temperatures from 10 to 40 °C, respectively. It is easy to see from the nature of these curves that active corrosion behavior is exhibited at each temperature and concentration of 84 disinfectant. And the polarization curves at 10 °C, 20 °C, 30 °C, 40 °C are quite similar. As can be seen from these figures, both the anodic and cathodic curves in the presence of 84 disinfectant are shifted to more positive direction compared with that in distilled water, suggesting that 84 disinfectant solution accelerates the corrosion of CRS in distilled water significantly. These figures also show that, with increasing concentration of 84-disinfectact from 0 to 20 mL/L, the anodic dissolution and cathodic reduction are speeded up clearly, then the anodic dissolution and cathodic reduction are slowed down quickly with increasing the ratio of 84-disinfectact from 20 to 100 mL/L compared to that of 20 mL/L. The result also indicates that the maximum acceleration of the reaction occurs at 20 mL/L 84 disinfectact.

It also can be seen from Figs.3a-d that some polarization curves in the presence of lower concentration of 84 disinfectact do not show sufficient linear Tafel regions. The distortion of the polarization curves is mainly caused by the solution resistance (solution ohmic drop) [22-24]. In order

to obtain meaningful data, it is necessary to perform an appropriate correction of polarization curves before the Tafel plot analysis.
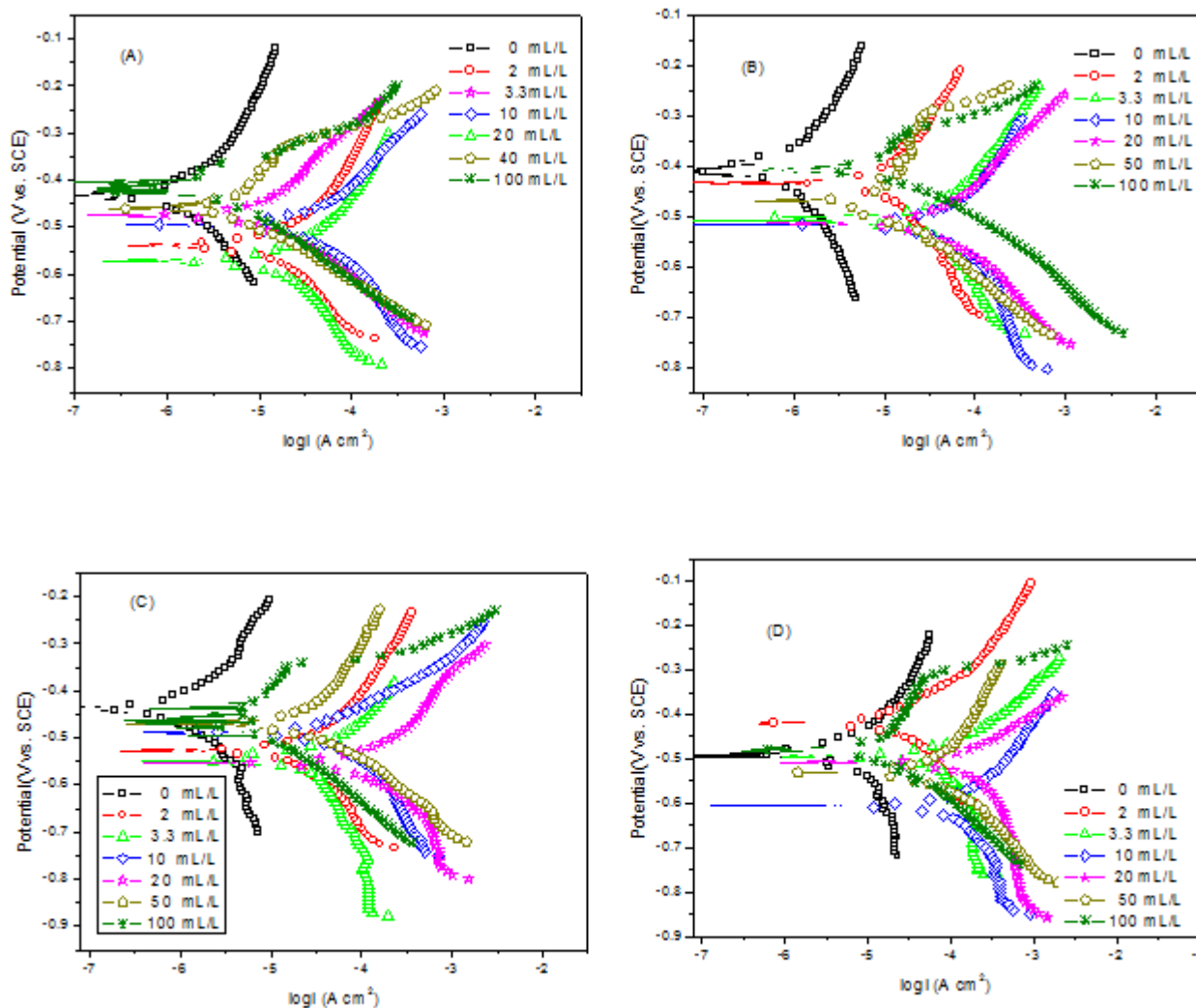

Figure 3. Tafel polarization curves for CRS with and without 84 disinfectant at different temperatures (A) 10 °C, (B) 20 °C, (C) 30 °C and (D) 40 °C.

The correction of polarization curves for ohmic drop was well performed according to the method described in literatures [17, 22-24] assuming that the experimentally applied overpotential at any current is given by the following equation:

$$E = \beta_a + \beta_c \ln i + iR_s \qquad (3)$$

where E is the applied overpotential vs. *SCE*, i the current density, R_s the solution resistance and β_a and β_c are respectively anodic and cathodic Tafel slopes.

Using the relationship (3), the following equation for correction of the polarization curves for ohmic drop can be obtained [17, 22]:

$$i = i_{corr} \left[\exp\left(\frac{E - E_{corr} - iR_s S}{\beta_a} \right) - \left(-\frac{E - E_{corr} - iR_s S}{\beta_c} \right) \right] \qquad (4)$$

where i_{corr} is the corrosion current density, E_{corr} the corrosion potential vs. *SCE* and *S* is the area of the exposed surface of the working electrode in cm^2.
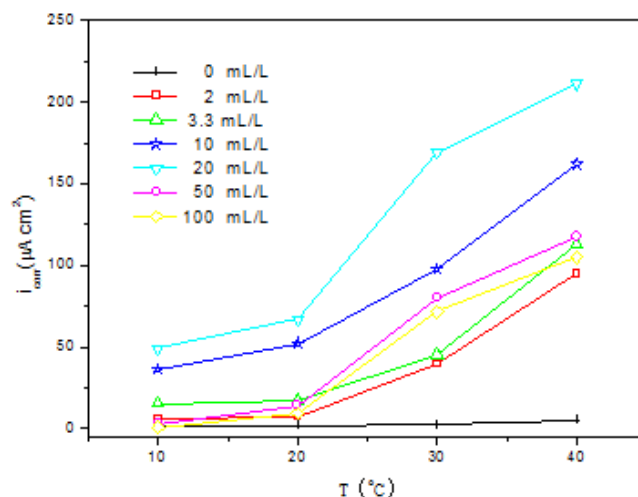

Figure 4. Relationship between corrosion current density (i_{corr}) and temperatures (T) in the absence and presence of 84-disinfectant.

Table 1. Polarization parameters for CRS in solutions with and without 84 disinfectant at 10 °C, 20 °C, 30 °C and 40 °C

| T (°C)	84-disinfectant (mL/L)	E_{corr} (mV vs. SCE)	i_{corr} (μA cm^{-2})	β_c (mV dec^{-1})	β_a (mV dec^{-1})
10	0	-432.9	1.7	192.8	209.0
10	2	-538.9	5.7	117.3	106.4
10	3.3	-571.9	15.3	145.6	116.9
10	10	-495.0	36.5	172.6	155.9
10	20	-475.9	48.9	106.6	171.1
10	50	-459.7	2.9	74.8	72.7
10	100	-421.1	0.5	21.5	48.7
20	0	-406.3	1.8	217.2	155.8
20	2	-433.3	7.4	109.1	124.9
20	3.3	-506.2	17.0	81.4	68.7
20	10	-516.6	52.3	173.8	199.7
20	20	-515.8	67.0	204.6	263.6
20	50	-470.4	14.1	78.6	72.7
20	100	-407.8	9.3	73.6	214.1
30	0	-438.8	2.3	198.2	192.4
30	2	-527.5	39.4	376.9	212.7
30	3.3	-541.0	45.3	687.6	138.3
30	10	-488.8	97.9	242.1	200.8
30	20	-553.3	169.4	262.9	219.2
30	50	-469.7	89.2	148.0	421.3
30	100	-462.6	71.4	136.2	297.6
40	0	-484.7	5.2	207.9	160.4
40	2	-417.4	18.0	151.2	121.0
40	3.3	-493.4	113.2	468.9	140.1
40	10	-603.9	162.0	421.0	150.9
40	20	-506.5	211.3	375.7	158.9
40	50	-530.8	117.6	191.9	487.2
40	100	-481.2	105.8	114.7	235.0

And the solution resistance (R_s) used in this paper is derived from EIS method which provides a variety of information on the parameters of the electrochemical cell and can be profitably used to determine the solution resistance [17, 22]. According to Eq.(4), more powerful non-linear least squares algorithm based on the Levenberg-Marqurdt Method (LEV) was used to fit the experimental data to obtain the corrosion current density (Icorr), Tafel slopes β_a and β_c.

To enhance the quality of fit, the data rage is set within E_{corr} vs. $SCE \pm 150$ mV, the initial values of E_{corr}, I_{corr}, β_a and β_c are set to 0 V, 10^{-5} A cm^{-2} and 120 mV decade^{-1}, respectively. Rather than giving equal importance to each data point, data points below the current accuracy which is chosen as 1×10^{-5} A m^{-2} in this paper have reduced importance in the overall goodness of fit. This causes the fit to place a higher importance on the data points with larger currents. In all cases, the above method fits the experimental curves well after correction for ohmic drop in the selected range. The potentiodynamic polarization parameters after correction for ohmic drop including E_{corr}, I_{corr}, β_a and β_c were listed in table 1.

In order to elucidate the corrosion regularities visually, Fig.4 also shows the relationship between corrosion current density (i_{corr}) and temperatures (T) in the absence and presence of 84 disinfectant. From table 1 and Fig.4 it can be easily seen that, at each same temperature, the corrosion current densities obviously increase with increasing concentration of 84 disinfectant from 0 to 20 mL/L, and then decreases in solution with 84 disinfectant level higher than the threshold value (20 mL/L). That is, the maximum corrosion occurs in the presence of 20 mL/L 84 disinfectant at each same temperature. Furthermore, at the same concentration the current densities increase with increase of the temperature. The results are in good agreement with that obtained from gravimetric measurements.

3.3. Electrochemical impedance spectroscopy (EIS)

The corrosion behaviors of CRS in solutions in the presence of different concentrations of 84 disinfectant at 30 °C were also investigated by the electrochemical impedance spectroscopy.
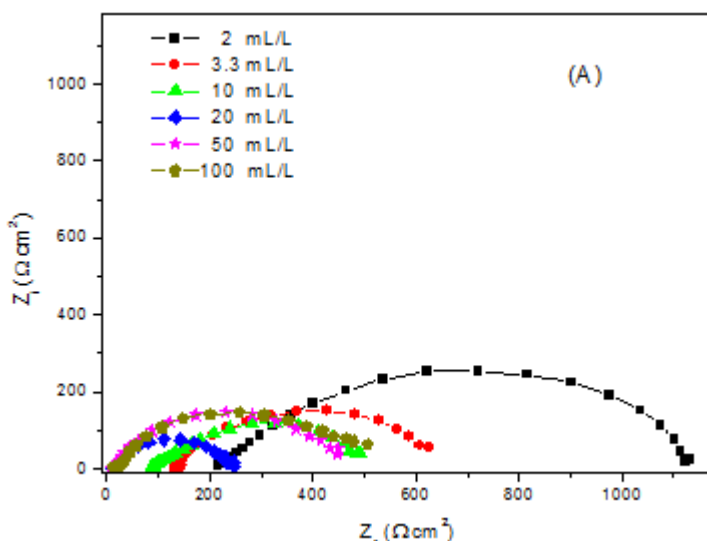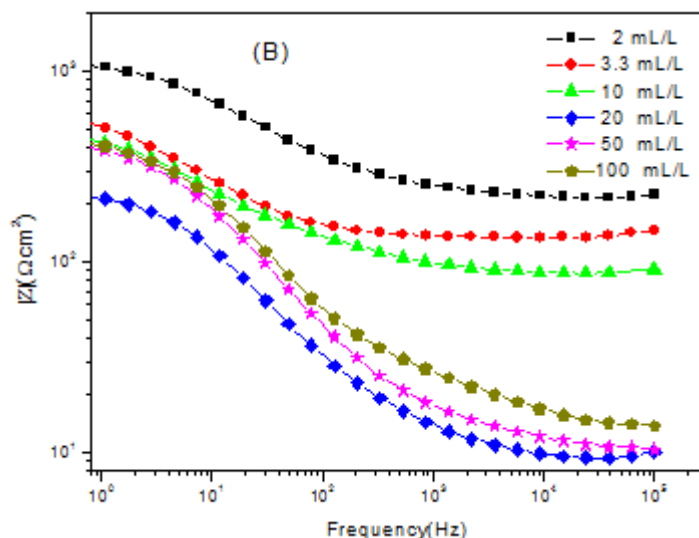
Figure 5. EIS of CRS in different concentration of 84 disinfectant after 2h immersion at 30 °C (A) Nyquist plots and (B) Bode plots.

Nyquist plots of CRS in solutions with 84 disinfectant were given in Fig. 5a. From Fig.5a it is clear that all impedance spectra exhibit a single depressed semicircle in general. These depressed incomplete semicircles can be attributed to the charge transfer that takes place at electrode/solution interface, and the transfer process controls the corrosion reaction of CRS [25]. From Fig.5a it is apparent that, with increasing the concentration of 84 disinfectant from 2 to 20 mL/L, the capacitance loop decreases, then it increases with increasing the concentration of 84 disinfectant from 20 to 100 mL/L, that is, the smallest capacitance loop appears at 20 mL/L 84 disinfectant, suggesting that the maximum corrosion rate appears at 20 mL/L 84 disinfectant.

Table 2. EIS parameters for CRS in 84 disinfectant solutions at 30 °C.

84 disinfectant (mL/L)	R_s (Ω cm^2)	CPE (μF cm^{-2})	α	R_t (Ω cm^2)
2	218.1	90	0.62	963.4
3.3	135.1	302	0.69	515.3
10	87	409	0.57	461.3
20	9.707	558	0.71	242.9
50	11.08	233	0.71	463.2
100	14.66	291	0.63	531.7

In order to interpret the Nyquist plots more concisely, the equivalent circuit shown in Fig. 6, with a solution resistance (R_s), a charge transfer resistance (R_{ct}) and a constant phase element (*CPE*), was proposed to simulate the results. The constant phase element (*CPE*) was usually used instead of a capacitance to account for the non-ideal capacitance response due to the almost complete absence of pure capacitance in the real electrochemical process [25-27]. R_s, R_{ct}, *CPE* value and the related CPE exponent (α) in the presence of different concentrations of 84 disinfectant at 30 °C were obtained using

ZSimpWin 3.10 software and listed in Table 2. Table 2 clearly shows that R_{ct} values decrease and C_{dl} values increase with increasing concentration of 84 disinfectant when concentration of 84 disinfectant is lower than 20 mL/L, and then R_{ct} values increase and C_{dl} values decrease quickly in solution with 84 disinfectant level higher than the threshold value (20 mL/L). The decrease in capacity (C_{dl}) after the threshold value may be attributed to the formation of a protective layer on the electrode surface with increasing 84 disinfectant concentration [28]. This suggests that protective film will form on CRS surface when 84 disinfectant concentration is higher or equal to 20 mL/L.

Moreover, the Bode plots of CRS in solutions with 84 disinfectant corresponding to Fig.5a were given in Fig. 5b. The impedance plots at higher frequency limit (100 kHz) in impedance plots correspond to the ohmic resistance of the film of corrosion products and the solution between the working electrode and reference electrode. At higher frequencies the impedance value |Z| does not fall to zero. This indicates the solution resistance remains between the reference and working electrodes [29]. In addition, according to Loren and Mansfeld [30], the corrosion resistance of samples is determined by R_p

$$R_p = \lim_{\varpi \to 0} R_e \{Z_f\}_{E=E_{corr}} \tag{5}$$

Where $R_e\{Z_f\}$ represents the real part of the complex faradic impedance, Z_f and ω correspond to the angular celocitt of A.C. signal ($\omega=2\pi f$ where f is frequency (Hz)). R_p corresponds to the horizontal line in a range of low frequencies on the Bode plots. In the case that Bode plots do show horizontal lines at low frequencies due to the limited low frequency range, the impedance modulus value |Z| at the lowest frequency in the Bode plots can be used to characterize the corrosion resistance [30-32]. It is clear that, the impedance modulus value |Z| at the lowest frequency (0.1Hz) first increases with decreasing 84 disinfectant concentration from 2 to 20 mL/L and then significantly increases with increasing 84 disinfectant concentration from 20 to 100 mL/L, which also indicates that the maximum corrosion rate appears at 20 mL/L 84-disinfectant.
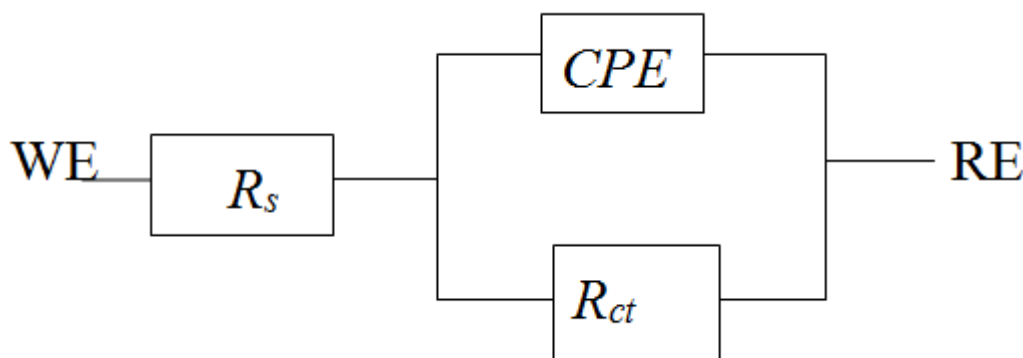
3.4. AFM studies

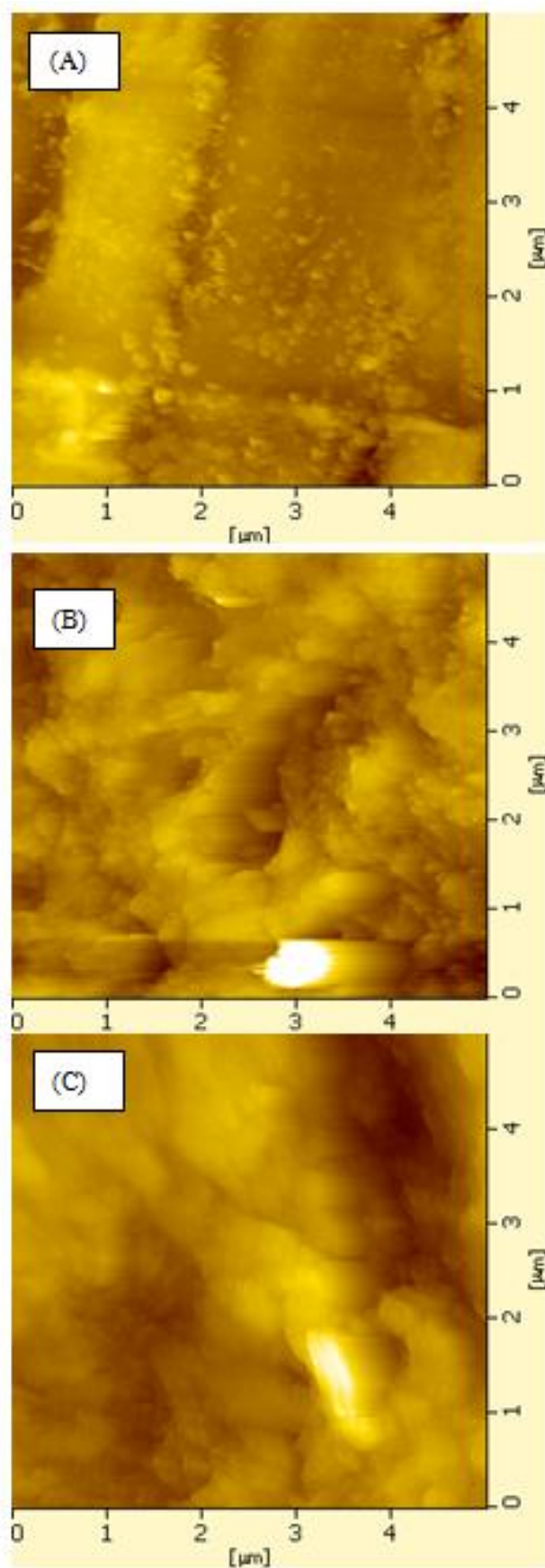**Figure 6.** Equivalent electrical circuit of EIS.

Figure 7. AFM surface topography images in solutions (A) in the absence of 84 disinfectant; (B) in the presence of 3.3 mL/L 84 disinfectant and (C) in the presence of 20 mL/L 84 disinfectant.
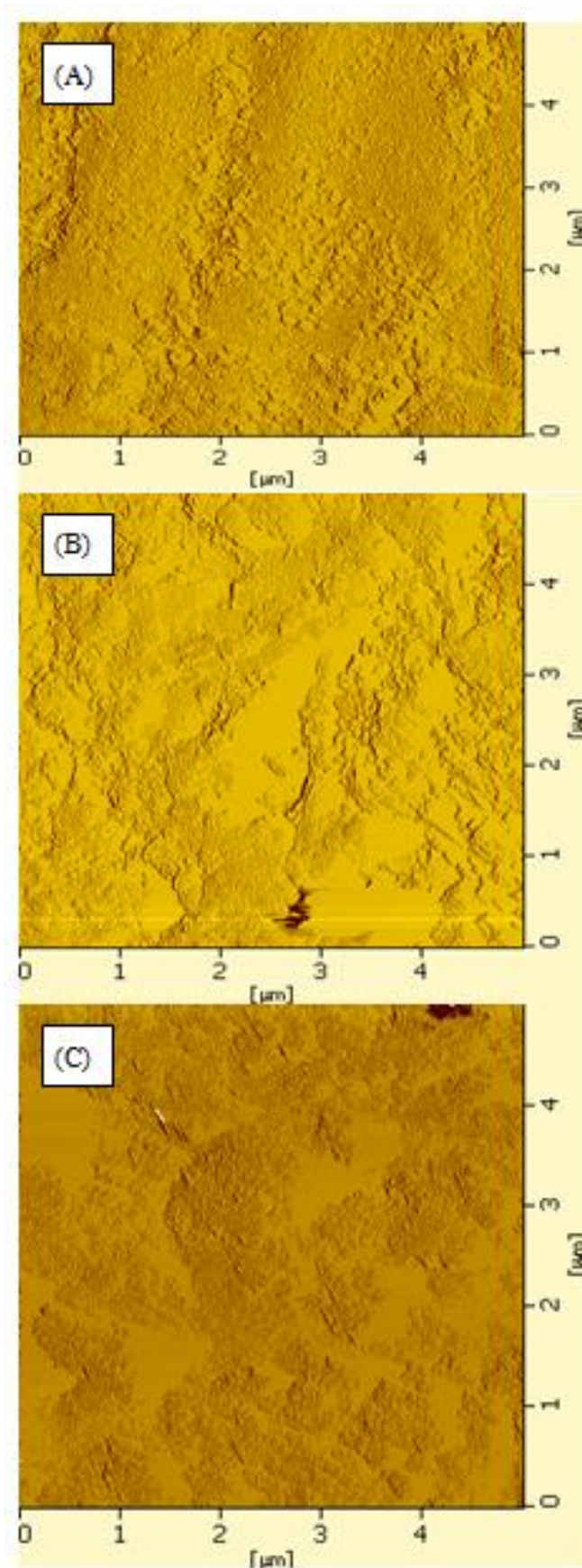
Figure 8. AFM two-dimensional images in solutions (A) in the absence of 84 disinfectant; (B) in the presence of 3.3 mL/L 84 disinfectant and (C) in the presence of 20 mL/L 84 disinfectant.
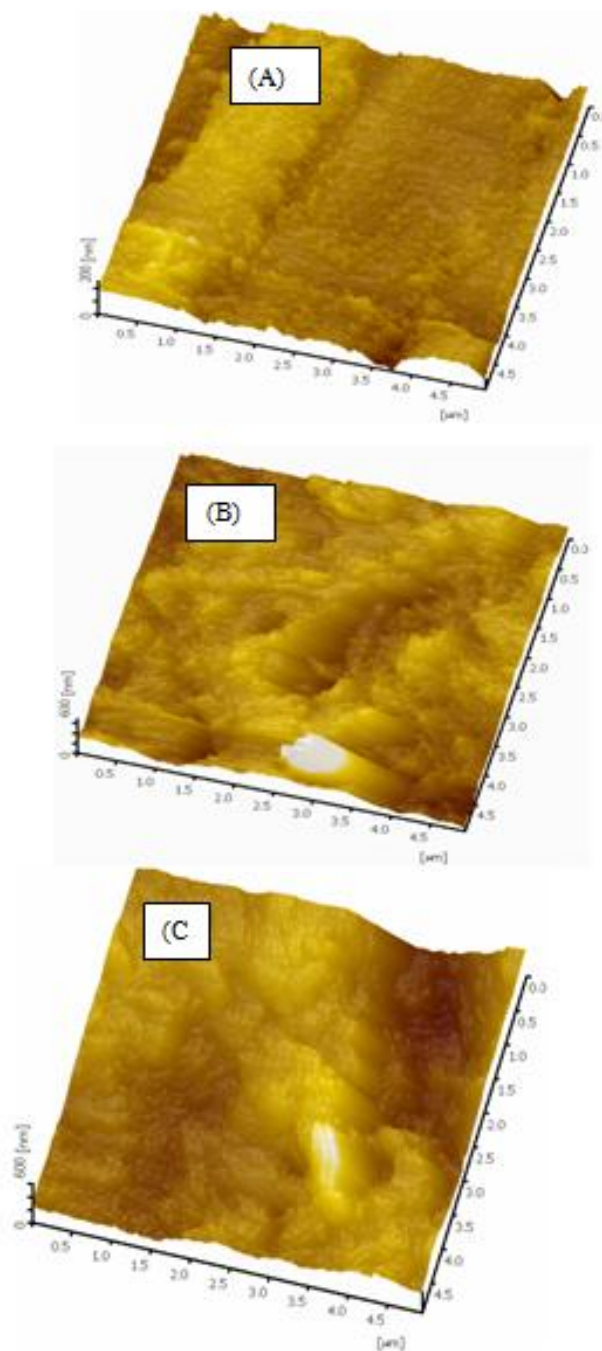
Figure 9. AFM three-dimensional images in solutions (A) in the absence of 84 disinfectant; (B) in the presence of 3.3 mL/L 84 disinfectant and (C) in the presence of 20 mL/L 84 disinfectant

AFM provides a powerful technique of investigating the surface microstructure [33-36]. In order to assess the surface microstructure, AFM surface topography images of CRS after immersion in solutions with and without 84 disinfectant for 4 h were shown in Fig.7, the corresponding two-dimensional images and three-dimensional images were showed in Figs. 8 and 9, respectively. The AFM images shown in Figs. 7–9 (A) are the corroded surface of CRS in the absence of inhibitors. From these pictures, it is clearly found that the surface is more uniform in character and there is little tendency towards local enrichment of products on the surface. In addition, parallel features in these

figures which can be associated with abrading scratches are also observed. Figs.7-9(B) show the corrosion surface of CRS after immersion in 3.3 mL/L 84 disinfectant solution, it is clearly found that the surface looks relatively uneven and appears potholed shape, suggesting that electrochemical corrosion are accelerated compared to that in the absence of 84-disinfectant. However, in the presence of 20 mL/L 84 disinfectant (Fig.7-9(C)), it seems that there are some corrosion products appeared on CRS surface, and the surface looks more flat and close than that in the presence of 3.3 mL/L 84 disinfectant, which reveals the formation of complete and protective film on CRS surface.

4. DISCUSSION

The present study shows that concentration of 84 disinfectant and temperature can affect the corrosion rate of CRS in solution significantly. According to chemical kinetics, the reaction rate depends on two factors: the frequency with which the reactive species collide and the fraction of these collisions which are effective and result in reaction. The reaction molecules which meet the above-mentioned factors increase with increasing temperature. Furthermore, the ions in solution move faster at higher temperature than those at lower temperature which results in increase of the solution conductivity at higher temperature. For reasons given above the corrosion rate of CRS in 84 disinfectant solution increases with increasing test temperature.

Also, the corrosion rate of CRS increases with increase of the concentration of 84 disinfectant in lower 84 disinfectant concentrations. As the active ingredient in 84 disinfectant, sodium hypochlorite takes part in the corrosion process and is reduced in the cathodic areas which is balanced by the anodic dissolution of CRS in 84 disinfectant.

$$Fe = Fe^{2+} + 2e \qquad\qquad\qquad (a)$$

$$ClO^- + H_2O + 2e^- = Cl^- + 2OH^- \qquad\qquad (b)$$

Therefore, countless electrochemical cells begin to form on the surface of CRS, with increasing the concentration of hypochlorite ions, the electrochemical corrosion will accelerate. It is well known that the standard cell potential for ClO^-/Cl^- is 0.89 V which is higher than the standard cell potential for Fe^{3+}/Fe^{2+} (0.771V), so Fe^{2+} can be further oxidized to Fe^{3+} by reduction of ClO^-.

$$2Fe^{2+} + ClO^- + H_2O = 2Fe^{3+} + Cl^- + 2OH^- \qquad (c)$$
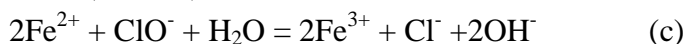
To make out the form of the Fe ions in 84 disinfectant solutions, a series of experiments were also carried out.

First, potassium ferrocyanide($K_4Fe(CN)_6$) was added to one part of 84 disinfectant solution, the solution became blue. This phenomenon indicated that Fe^{3+} ions existed in 84-disinfectant.
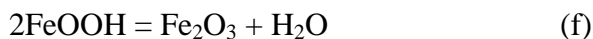
Then, potassium ferricyanide ($K_3Fe(CN)_6$) was added to another part of 84 disinfectant solution, however, the solution did not become blue which indicated that Fe^{2+} ions could not be in 84 disinfectant solution.

Hence, the Fe^{3+} ions are the dominant corrosion products of CRS dissolved in 84 disinfectant solutions, which can be related to the strong oxidation of 84-disinfectant.

From reaction (b) it is easy to see that the concentration of hydroxyl ions (OH^-) will increase with increasing concentration of 84 disinfectant, but the following reactions will occur when the concentration of hydroxyl ions is increased to a certain level.

$$Fe^{3+} + OH^- = Fe(OH)_3 \qquad (d)$$

$$Fe(OH)_3 = FeOOH + H_2O \qquad (e)$$
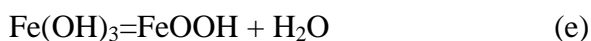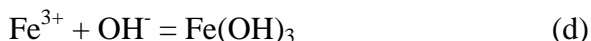
Then FOOH will gradually transform to more stable substance, Fe_2O_3

$$2FeOOH = Fe_2O_3 + H_2O \qquad (f)$$

The more the amount of 84 disinfectant presents in solution, the more quickly the above reactions go on. $FeOOH$ and Fe_2O_3 are insoluble in weak basic solution. The formation of these insoluble substances will form a barrier film on CRS that may counteract the further migration of the ions. Therefore the electrochemical corrosion rate will slow down to some extent when concentration of 84 disinfectant is increased to a certain level.

5. CONCLUSION

1. 84 disinfectant can accelerate the corrosion of CRS clearly. Concentration of 84 disinfectant and temperature affect the corrosion of CRS significantly. With increasing test temperature at each same concentration, the corrosion rate increases clearly, but the corrosion rate does not increase with increasing concentration of 84 disinfectant all the way, the maximum corrosion rate appears at solution in the presence of 20 mL/L 84 disinfenctant at each temperature.

2. The Fe^{3+} ions are the dominant corrosion products dissolved in 84 disinfectant solutions due to the strong oxidation of 84 disinfectant.

3. After concentration of 84 disinfectant is increased to a certain level, with reactions going on, $FeOOH$ and Fe_2O_3 will form a barrier film on CRS surface and slow down the corrosion rate to some extent.

References

1. Y. Li, M.B. Ives, K.S. Coley, J.R. Rodda, *Corros. Sci.* 2004, 46, 1969.
2. U. Kivisäkk, *Corros. Sci.* 2003, 45, 485.
3. Z. Panossian, N. L. de Almeida, R. M. F. de Sousa, G. de Pimenta, L. B. S. Marques, *Corros. Sci.* 2012, 58, 1.
4. F. Nagies, K.E. Heusler, *Electrochim. Acta* 1998, 43, 41.
5. I. Sekine, H. Ohkawa, T. Handa, *Corros. Sci.* 1982, 22, 1113.
6. D.D.N. Singh, R. Ghosh, B.K. Singh, *Corros.Sci.* 2002, 44, 1713.
7. R.E. Melchers, *Corros. Sci.* 2003, 45, 2609.
8. I. Gurrappa, G. Malakondaiah, *Mater. Sci. Eng. A −Struct.* 2005, 391, 235.
9. L. Feng, H. Yang, F. Wang, *Electrochim. Acta* 2011, 58, 427.

10. Y. G. Avdeev, Y. I. Kuznetsov, A. K. Buryak, Corros. Sci. 2013, 69, 50.
11. E. S. Meresht, T. S. Farahani, J. Neshati, *Corros. Sci.* 2012, 54, 36.
12. L. Li, Q. Qu, W. Bai, F. Yang, Y. Chen, *Corros. Sci*. 2012, 59, 249.
13. X. Li, S. Deng, H. Fu, *Corros. Sci.* 2011, 53, 3241.
14. Q. Qu, Z. Hao, S. Jiang, L. Li and W. Bai, *Mater. Corros.* 2008, 59, 883.
15. Q. Qu, G. Gao, H. Guo, L. Li and Z. Ding, *Mater. Corros.*2011, 62, 778.
16. Q. Qu, L. Li, S. Jiang, W. Bai, Z. Ding, *J. Appl. Electrochem.* 2009, 39, 569.
17. Q. Qu, L. Li, S. Jiang, W. Bai, Z. Ding, *Corros. Sci.* 2009, 51, 2423.
18. Z. Tan,Y.Xu, *Modern Preventive Medicine.*2006, 33, 1938.
19. J.L. Sagripanti, A. Bonifacino, *Am. J. Infect. Control* 1996, 24, 364.
20. F. Chen, W. Li, Q. Xu, *Chinese J. Disinfect.* 2008, 25, 320.
21. X.C. Fu, W.X. Shen, T.Y. Yao, Physical Chemistry, Higher Education Press, Beijing, 2000.
22. L.A. De Faria, J.F.C. Boodts, S. Trasatti, *J. Appl. Electrochem.* 1996, 26, 1195.
23. N.T. Krstajic, S. Trasatti, *J. Appl. Electrochem.* 1998, 1291.
24. A. Kapalka, G. Fóti, C. Comninellis, *Electrochem. Commun.* 2008, 0, 07.
25. M. Lebrini, M. Lagrenee, H. Vezin, M. Traisnel, F. Bentiss, *Corros. Sci.* 2007, 49, 2254.
26. G.H. Cartledge, Br. Corros. J. 1966, 1, 293.
27. A. Pilbáth, L. Nyikos, I. Bertóti, E. Kálmán, *Corros. Sci.* 2008, 50, 3314.
28. K. Tanno, M. Itoh, H. Sekiya, H. Yashiro, N. Kumagai, *Corros. Sci.* 1993, 34, 1453.
29. D. K. Yadav, M. A Quraishi; B. Maiti, *Corros. Sci.* 2012, 55, 254.
30. D.J. Loren, F. Mansfeld, *Corros. Sci.* 1981, 21, 647.
31. D.Q. Zhang, L.X. Gao, G.D. Zhou, *J. Appl. Electrochem.* 2003, 33, 361.
32. G.W. Walter, *Corros. Sci.* 1986, 26, 681.
33. Q. Qu, S.Jiang, W.Bai, L.Li, *Ecectrochim. Acta* 2007, 52, 6811.
34. S. Garcia-Manyes,G. Oncins, F. Sanz, *Electrochim. Acta* 51(2006)5029-5036.
35. D. Grujicic, B. Pesic. *Electrochim. Acta* 2006, 51, 2678.
36. A.M.C. Paquim, T.S. Oretskaya, A.M.O. Brett, *Electrochim. Acta* 2006, 51, 5037.